Orbital Insulators and Orbital Order-disorder Induced Metal-Insulator Transition in Transition-Metal Oxides

Dong-Meng Chen[1,2] and Liang-Jian Zou[1]

1 Key Laboratory of Materials Physics,

Institute of Solid State Physics, Chinese Academy of Sciences,

P. O. Box 1129, Hefei 230031, China and

2 Graduate School of the Chinese Academy of Sciences

(Dated: February 2, 2008)

Abstract

The role of orbital ordering on metal-insulator transition in transition-metal oxides is investigated by the cluster self-consistent field approach in the strong correlation regime. A clear dependence of the insulating gap of single-particle excitation spectra on the orbital order parameter is found. The thermal fluctuation drives the orbital order-disorder transition, diminishes the gap and leads to the metal-insulator transition. The unusual temperature dependence of the orbital polarization in the orbital insulator is also manifested in the resonant x-ray scattering intensity.

KEYWORD: Orbital ordering, metal-insulator transition, orbital insulator, resonant X-ray scattering

I. INTRODUCTION

Metal-insulator transition (MIT) in strongly correlated transition-metal oxides (TMO) is one of the central problems in condensed matter physics, it has attracted extensive attention in recent decades since it has been found that high temperature superconductivity, colossal magnetoresistance and many other phenomena occur in the vicinity of MIT[1,2]. These strongly correlated electronic systems exhibit very complicated and rich phase diagrams with temperature, doping, pressure and magnetic field [3,4]. In these compounds, the temperature induced MIT in V_2O_3 and manganites is especially interesting, because the MIT temperature T_M is much smaller than the insulating gap (Δ) in transport, for example in V_2O_3, T_M=154 K$<<\Delta = 0.6$ eV[5]. Obviously, the thermal fluctuation is not the driven force of the MIT. It has recently realized that the orbital degree of freedom and orbital ordering (OO) play important roles in the groundstate (GS) properties of these TMO.

The OO was first proposed to explain the complicated magnetic structures by Kugel et al. [6] for $KCuF_3$ and by Castellani et al. [7] for V_2O_3. Due to the strong correlation between $3d$ electrons and the large anisotropy of the $3d$ wavefunctions, the orbital degree of freedom and the OO affect many electronic and magnetic properties of these strongly correlated systems [4,6−9], and have been extensively studied in colossal magnetoresistive manganites, vanadium oxides and many other TMO [for example, see Ref.10]. Experimentally orbital order-disorder transition is usually accompanied by MIT, such as in prototype MIT compound V_2O_3, an obvious insulator to metal transition occurs at T_M=T_C [11], here T_C is the Curie-Weiss temperature. It is believed that in V_2O_3, the OO transition (OOT), the MIT and the magnetic transition occur simultaneously, i.e. $T_M = T_{OO} = T_C$ [12]. We also notice that in lightly doped $La_{0.88}Sr_{0.12}MnO_3$ the ferromagnetic insulator to ferromagnetic metal transiting at T_M is identified as an OOT by Endoh et al [13], or, $T_M = T_{OO}$, ruling out the significant role of cooperative Jahn-Teller (JT) distortion on the GS. The orbital phase transition near the vicinity of MIT is also reported in $La_{1-x}Ca_xMnO_3$ ($x \approx 0.2$) [14]. These experiments clearly establish a close relationship between OOT and MIT. Theoretically Castellani et al. first suggested the correlation between OOT and MIT in V_2O_3 [7], they proposed that the MIT associated with the OO was driven by the variation of the entropy in the presence of long-range magnetic and orbital orders. Khaliullin et al. [15] attributed this correlation to the formation of orbital polaron. Nevertheless, it is not well understood theoretically how

the OO insulator evolves to MIT with lifting temperature.

In this paper, we demonstrate that the strong orbital correlation in TMO with orbital degenerate 3d electrons leads the GS to be an orbital insulator, and the orbital order-disorder driven MIT. Starting from a twofold-degenerate spin-orbital interacting model, and using the cluster self-consistent field (cluster-SCF) approach developed recently, we first determine the OO GS; and then show that the insulating gap of the single-particle spectrum opens as the long-range OO establishes. With increasing temperature, the thermal fluctuation drives OOT, also the energy gap of the single-particle excitation vanishes at T_{OO}, indicating the transition from insulator to metal. The resonant X-ray scattering (RXS) intensity diminishes to zero near the critical temperature T_{OO}. The rest of this paper is organized as follows: in Sec.II we describe the effective model Hamiltonian of an orbital insulator and the cluster-SCF approach; then we present the magnetic and orbital structures in GS, the T-dependent OO parameters and the gap of single-particle excitation spectra in Sec.III; the variation of the temperature and the azimuthal angle dependence of the RSX intensity are given in Sec.IV, and the last section is devoted to the remarks and summary.

II.   MODEL HAMILTONIAN AND METHOD

In many perovskite transition-metal oxides under the octahedral crystalline field, the five-fold degenerate 3d orbits of the transition metal ions split into lower t_{2g} and higher E_g orbits. For clarification and simplification we consider such an ideal cubic TMO system that the t_{2g} orbits are filled and contribute no spin, and the twofold degenerate E_g orbits are occupied by one hole or one electron, corresponding to the electron configuration of $3d^9$ in $KCuF_3$ or $3d^7$ in $LaNiO_3$. Such a system is spin-1/2 and twofold orbital degenerate, or the orbital pseudospin τ=1/2. We denote the two E_g orbits as $|1\rangle=|e_{g1}\rangle=|d_{3z^2-r^2}\rangle$ and $|2\rangle=|e_{g2}\rangle=|d_{x^2-y^2}\rangle$. The major low-energy physics of the system is described by the twofold-degenerate Hubbard model with strong Coulomb interaction [6,7]. In the second-order perturbation approximation the E_g electrons interact with each other through the low-energy superexchange coupling, which is expressed as:

$$H_{SE} = \sum_{\substack{\langle ij \rangle_l \\ l=x,y,z}} (J_1 \vec{s}_i \cdot \vec{s}_{j_l} + J_2 I_i^l \vec{s}_i \cdot \vec{s}_{j_l} + J_3 I_i^l I_{j_l}^l \vec{s}_i \cdot \vec{s}_{j_l}$$

$$+ J_4 I_i^l I_{j_l}^l) \tag{2.1}$$

where the operator $I_i^l = \cos(2\pi m_l/3)\tau_i^z - \sin(2\pi m_l/3)\tau_i^x$, the index l, $l = x, y$ or z, denotes the direction of a bond; $\langle ij \rangle_l$ connects site i and its nearest-neighbor site j along the l direction, and $(m_x, m_y, m_z) = (1,2,3)$. τ^z and τ^x are the Pauli matrix, $\tau^z = \frac{1}{2}$ represents the orbital polarization in the state $|1\rangle$ and $\tau^z = -\frac{1}{2}$ the orbital polarization in the state $|2\rangle$. Thus the polarization degree of the orbit, $\langle \tau \rangle$, is called the orbitalization. The constants J_1, J_2, J_3 and J_4 are the superexchange interactions, and are read: $J_1 = 8t^2 \left[U/(U^2 - J_H^2) - J_H/(U_1^2 - J_H^2) \right]$, $J_2 = 16t^2 \left[1/(U_1 + J_H) + 1/(U + J_H) \right]$, $J_3 = 32t^2 \left[U_1/(U_1^2 - J_H^2) - J_H/(U^2 - J_H^2) \right]$, and $J_4 = 8t^2 \left[(U_1 + 2J_H)/(U_1^2 - J_H^2) + J_H/(U^2 - J_H^2) \right]$, with $U = U_1 + 2J_H$, here $4t$ is the hopping integral between the $|2\rangle$ orbits along the z direction. U and U_1 are the intra- and inter-orbital Coulomb interactions, and J_H is the Hund's rule coupling. In this paper we adopt $t = 0.1$ eV and $J_H = 0.9$ eV.

Clearly, the fourth term in Eq.(1) is an orbital frustration interaction: while the exchange along the z direction stabilizes the alternating $|3z^2 - r^2\rangle$ and $|x^2 - y^2\rangle$ configuration, the equivalent coupling along the x or the y directions favors other orbital pair configuration, i.e. $|3x^2 - r^2\rangle$ and $|y^2 - z^2\rangle$ or $|3y^2 - r^2\rangle$ and $|z^2 - x^2\rangle$. The second term in Eq.(1) is a "magnetic field" for the orbital pseudospin, i.e. the orbital field. Due to the relation $I_i^x + I_i^y + I_i^z = 0$, the orbital field favors a peculiar orbital polarization and suppresses the orbital quantum frustration. However, if the spin correlations $\langle \vec{s}_i \vec{s}_j \rangle$ are identical along the x, y and z-directions, such as in the ferromagnetic (FM) or the *Neel* antiferromagnetic (G-type AFM) ordered structure, the orbital field vanishes. Then the third spin-orbital interaction, which are equal along the x, the y and the $z$directions, together with the fourth term leads to the strong quantum fluctuations and results in an orbital disordered ground state [9]. Fortunately, the conventional JT instabiity lowers the cubic symmetry to the tetragonal symmetry through the JT distortion and lifts the orbital degeneracy. The tetragonal crystalline field, $\hat{H}_z = E_z \sum_i \tau_i^z$, is an additional orbital field to break the symmetry of orbital space, and favors a peculiar orbital configuration. Thus the full Hamiltonian including the crystalline field term is read:

$$\hat{H} = \hat{H}_{SE} + \hat{H}_z. \tag{2.2}$$

We will discuss the cooperative JT effect on the OO in the Sect.V.

It is still a difficult task to treat the spin and orbital correlations and fluctuations, and to find the GS of Eq.(2) with high accuracy. To study the GS properties of these TMO systems,

we recently developed the cluster self-consistent field (cluster-SCF) approach to study the OO properties and the evolution of GS properties with interaction parameters in V_2O_3 [16]. This approach combines the exact diagonalization and the self-consistent field techniques, the main idea is briefly addressed as follows: firstly, choose a proper cluster, usually the unit cell of the TMO compound. Secondly, divide the interactions in Eq.(2) into two types: the internal bond interactions, H_{ij}, between the sites R_i and R_j in the cluster, and the external bond interactions, H'_{il}, between the environment site R_l and the site R_i in the cluster. The periodic condition enforces the electronic states at the environmental site R_l to be identical to the corresponding atom inside the cluster. After diagonalizing the internal interaction H_{ij} of the cluster, the interactions of the environment site R_l in H'_{il} acting on the cluster are obtained as a initial value of the self-consistent field (SCF): $h'_i=Tr_l(\rho_{il}H'_{il})$, here ρ_{il} is the reduced density matrix of the bond $\langle il \rangle$ after tracing over all of the other sites in the cluster. Thirdly, diagonalize the cluster Hamiltonian H_{ij} in the presence of the SCF h'_i. Iteration is then performed until the orbital correlation functions and the SCF h'_i converge. The GS properties of the system and the effective field of the surrounding atoms applied on the inside atoms of the cluster are thus obtained. One of the advantages of the present approach is that the short-range correlation of the spins and the orbits, which is neglected in the conventional self-consistent mean-field method, is taken into account.

To check the validity and convergence of the cluster-SCF approach, we apply it on the simple spin-1/2 AFM Heisenberg model. The Hamiltonian is read:

$$H = J\sum_{\langle ij \rangle} \vec{s}_i \cdot \vec{s}_j \qquad (2.3)$$

where $\vec{s}_i$ is the operator for the $i-th$ spin and $J > 0$. In our numerical calculation code, the convergence of the GS energy is considered as the truncation condition of iterations, when the relative error of the GS energy between two iterations is within 10^{-8}, the GS energy is converged. The net nearest-neighbor spin correlation function $S(\vec{s}_i, \vec{s}_j)=\langle \vec{s}_i \cdot \vec{s}_j \rangle - \langle \vec{s}_i \rangle \cdot \langle \vec{s}_j \rangle$ and the spin polarization $\langle s_z \rangle$ are used cooperatively to determine the magnetic structure. We find $S(\vec{s}_i, \vec{s}_j)=-0.1115$ along the three axes, and the spin polarizations of lattice clearly falls into two distinct kinds: $\langle s_z \rangle=-0.4683$, and $\langle s_z \rangle=0.4683$. Obviously the GS is the *Neel* AFM structure, and the averaged spin deviation of the z component from 1/2 at each site is 0.0317, smaller than Anderson's zero-point fluctuation result 0.078 [17]. This difference is attributed to the lack of the long-range quantum fluctuation of the spins in our approach,

the present cluster-SCF approach includes only the short-range quantum fluctuations. This result clearly confirmed the efficiency and validity of our approach.

III. ORBITAL TRANSITION INDUCED METAL-INSULATOR TRANSITION

In this section we first utilize the cluster-SCF method to find the magnetic and orbital GS of Eq.(2), then explore the evolutions of the ordered orbital parameter and the energy gap of single-particle excitation spectra with increasing temperature in the strong correlation limit.

A. Magnetic and orbital structures in ground state

In many three-dimensional TMO the magnetic structure s are not difficult to determine by the neutron scattering and other experimental techniques, in the following in accordance with the spin configuration in the experiments, we treat the large local spins as semiclassical to save computation time, and focus on the orbital fluctuation and the orbital GS for various magnetic orders. To determine the most stable magnetic and orbital GS structure of Eq.(2), we choose a cubic 8-site cluster. In the cluster, each site has three internal bonds and three external bonds. The total energy of the cluster as a function of the ratio U/J_H for various
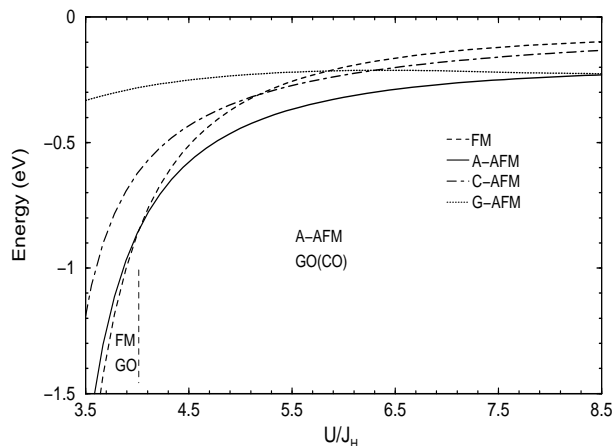

FIG. 1: Dependence of the total energy on the ratio U/J_H for different magnetic structures. CO and GO denote the C-type and *Neel* antiferro-orbital ordered structures, respectively. Theoretical parameters: $J_H = 0.9eV$ and $t = 0.1eV$, $E_z = -5meV$.
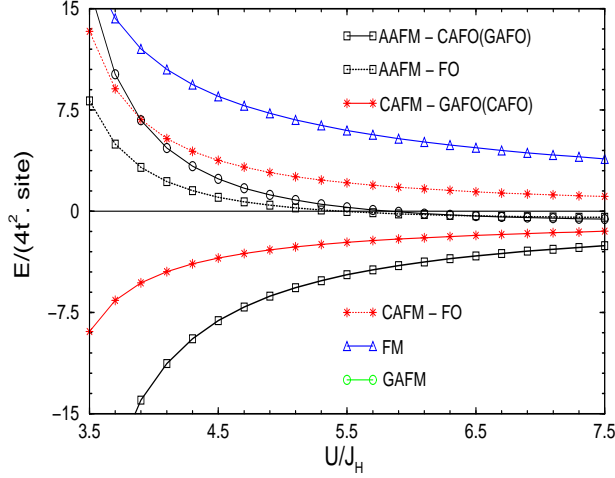
FIG. 2: Dependence of GS energy on the ratio U/J_H in the classical approximation. A-AFO denotes the A-type antiferro-orbital ordered structure. Theoretical parameters are the same to Fig.1

magnetic structures is shown in Fig.1. It is found that for small U/J_H, the GS is FM, which agrees with the mean-field results of Roth [18] and Cyrot and Lyon-Caen's [19]; while the GS is A-type AFM (A-AFM) for large U/J_H, i.e. AFM coupling along the c-axis and FM couplings in the ab-plane. In contrast, the classical approximation, which treats both the spin and the orbital operators as classical, shows that the GS is A-type AFM structure (A-AFM) over very wide U/J_H range, as seen in Fig.2. This classical result is in agreement with Kugel and Khomskii's result [6]. As we will show later, after taking into account the quantum effect, the orbital occupation and polarization are slightly different from the classical results.

To find the different stable magnetic structure sand the corresponding orbital configurations in different U/J_H range, we take the net orbital-orbital correlation function, $C_{ij} = \langle \vec{\tau}_i \cdot \vec{\tau}_j \rangle - \langle \vec{\tau}_i \rangle \cdot \langle \vec{\tau}_j \rangle$, together with the orbitalization $\langle \vec{\tau} \rangle$ to determine the orbital GS. In the FM phase, the Ising-like orbital-orbital interactions, $I_i^l I_{jl}^l$, which are identical for $l = x, y$ and z, as we analyzed in Sec.II, favors the orbital liquid GS. The tetragonal crystalline field suppresses the quantum fluctuations, drives the electrons into the $|3z^2 - r^2\rangle$ orbit in $E_z < 0$, and stabilizes the GS as G-type antiferro-orbital (AFO) ordering, which is most favorable of the the anisotropic distribution of the electron clouds. This agrees with the empirical Goodenough-Kanamori rules [20]. Our numerical results further show that all of the orbital correlations, S_{ij} along the x, y and z-directions, are AFO, thus each site is AFO

polarized with respect to its nearest-neighbor sites. One finds that the orbital occupations in the two sublattices are the combinations of $|1\rangle$ and $|2\rangle$: $\left(\sqrt{21}|1\rangle + \sqrt{19}|2\rangle\right)/\sqrt{40}$, and $\left(\sqrt{21}|1\rangle - \sqrt{19}|2\rangle\right)/\sqrt{40}$, for U/J_H=4.0 and $E_z = -5meV$.

With the increasing of U/J_H, the electronic superexchange interaction becomes small, in comparison with the crystalline field splitting, and more and more electrons occupy the $|x^2 - y^2\rangle$ orbit. The FM phase becomes unstable and transits to the AFM GS at $(U/J_H)_c$=4.1. At U/J_H=6.0, the orbital occupations in the two sublattices are approximately $\left(\sqrt{3}|1\rangle + |2\rangle\right)/2$ and $\left(\sqrt{3}|1\rangle - |2\rangle\right)/2$, as shown in Fig.3. The single-bond coupling energy, which is calculated
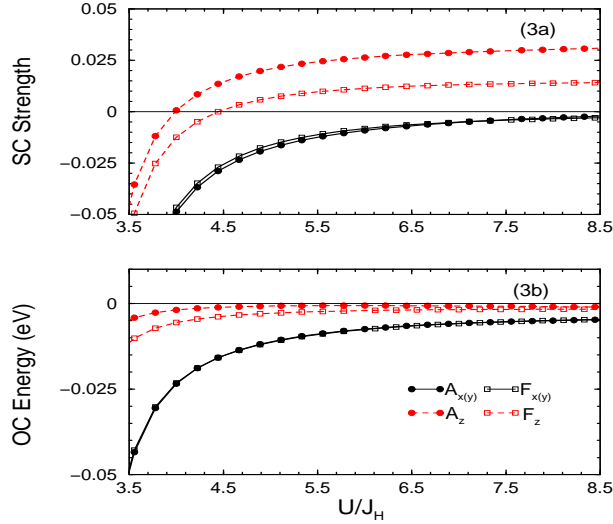

FIG. 3: Single-bond spin coupling (SC) strength (3a) and orbital coupling (OC) energy (3b) as the function of U/J_H for FM and A-AFM structures. $F_{x(y,z)}$ and $A_{x(y,z)}$ denote the x (y, z) bonds in the FM and the A-AFM structures, respectively.

for specific spin configuration via $E_{ij}^s = Tr_s(\rho_{ij}H_{ij})$, consists of the orbital-dependent spin coupling energy and the pure orbital coupling energy. It is found in Fig.3a and Fig.3b that for small U/J_H, the FM structure is the most stable, and the quantum fluctuation of spins is small; On the contrary, the A-AFM structure is the most stable for large U/J_H, addressing the GS orbital configuration in typical OO compound $KCuF_3$. In the following we focus the small U/J_H case. More detail results for large U/J_H and the effect of crystalline field splitting on OO compound $KCuF_3$ will be presented in a further paper.

The orbital phase transitions with the variation of the Coulomb interaction are typical quantum phase transitions. We find that the concurrence of two nearest-neighbor pseu-

dospins critically changes at the quantum transition point, detail result about how the entanglement of the orbital states evolves with the quantum phase transition will be published in the future. On the other hand, if we freeze the orbital configuration as the G-AFO ordered phase and to search the most stable spin configuration, we find that the magnetic structure transition from FM to A-AFM also occurs at the same critical value $(U/J_H)_c$=4.1, confirming the validity of the orbital GS.

B.   Temperature dependence of orbital order parameter

After determining the orbital GS, we explore the influence of the thermal fluctuations on the spin and orbital order parameters. At finite temperature T, thermal fluctuations exciting spin waves and orbital waves weaken both the orbital and the spin orderings, and destroy the magnetic order at the Curie temperature T_C and the OO at the orbital critical temperature T_{OO}. Since the spin order interplays with the OO, the reduction of spontaneous magnetization with increasing temperature also softens the orbital interaction, and *vice versa*. In the following we present the temperature dependence of the magnetic order and the OO parameters in small U/J_H range ($U/J_H<$ 4.1) in the conventional mean-field approximation. In the FM and G-AFO phase, the mean-field Hamiltonian is approximated as:

$$H_{MF} = \sum_i \left(J^z_{A(B)} \tau^z_{iA(B)} + J^x_{A(B)} \tau^x_{iA(B)} + J_s s^z_i \right) \tag{3.1}$$

where the coefficients $J^z_{A(B)}$, $J_{A(B)^x}$ and J_s depend on the magnetic order and the OO parameters, for example:

$$J_s = 3J_1 \left\langle s^z \right\rangle + 3/2 J_3 \left\langle s^z \right\rangle \left(\left\langle \tau^z_A \right\rangle \left\langle \tau^z_B \right\rangle + \left\langle \tau^x_A \right\rangle \left\langle \tau^x_B \right\rangle \right) \tag{3.2}$$

etc. In the FM and G-AFO phase, the thermal averages of the spontaneous magnetization and the orbital polarization, i.e. the orbitalization, satisfy the following self-consistent equations:

$$\left\langle s^z_a \right\rangle = Tr\{ s^z_a \exp\left(-\beta J_{sa} s^z_a \right) \}/Z^s_a \tag{3.3}$$

$$\left\langle \tau^{x(z)}_A \right\rangle = Tr\{ \tau^{x(z)}_A \exp\left(-\beta J^{x(z)}_A \tau^{x(z)}_A \right) \}/Z^{x(z)}_A \tag{3.4}$$

where β=$1/k_B T$. Also, the self-consistent equations for the A-AFM and G-AFO phase at large U/J_H can be obtained, but are more complicated. The temperature dependence of the spin and OO parameters for the system with small U/J_H is shown in Fig.4.

9

At low temperature, the magnetization and the two components of the orbitalization are nearly saturated. At lifting temperature $T > T_C/2$, the magnetization decreases considerably, while the orbitalization $\langle \tilde{\tau} \rangle$ almost does not change. With the temperature approaching T_C, the magnetization rapidly falls to zero, and the magnetic transition is obviously the first order, which originates from the strong anisotropy of the spin-orbit coupling, in agreement with T. M. Rice's argument based the Landau phenomenal theory for multiple parameter orders [22] and our renormalization group analysis to the critical indexes of the spin-orbital interaction models [23]. Meanwhile the OO parameter steeply diminishes a fraction at T_C, as observed in Fig.4. With further increasing in temperature, the OO parameter gradually decreases and finally vanishes at T_{OO}, with the characters of the second-order phase transition.

Due to the existence of orbital-orbital interaction in Hamiltonian (1), the long-range orbital correlation still exists after the magnetic order disappears. Therefore the orbital order-disorder transition temperature T_{OO} is higher than the magnetic transition temperature T_C, as observed in Fig.4. It is worthwhile noticing that the orbitalization components $\langle \tau^z \rangle$ and $\langle \tau^x \rangle$ display considerable discontinuity at the Curie temperature T_C, which indicates the strong correlation between the spin and the orbital degrees of freedom. The falling fraction of the orbitalization near T_C is about 12% with respect to the saturated magnitude. The *ab initio* electronic structure calculations based on the local density approximation with
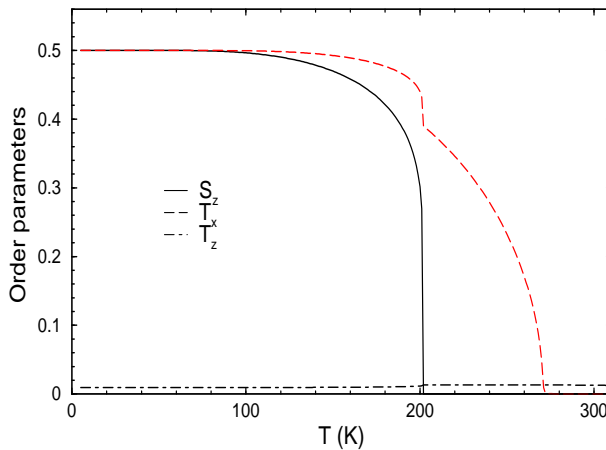

FIG. 4: Temperature dependence of the magnetization s_z, the orbital polarizations τ_z and τ_x. Theoretical parameters: $U = 3.6eV$, $J_H = 0.9eV$, $t = 0.1eV$.

correlation correction (LDA+U) have shown that in $KCuF_3$ the variation of the orbitaliza-

tion from the low-temperature AFM phase to the high-temperature paramagnetic phase is small, about 5% to 10% [24]. Experiments, however, showed the variation of the orbitalization is about 50% or even 100% in KCuF$_3$ [22] and in V$_2$O$_3$ [25]. This discrepancy may arise from two reasons: the first one is that the paramagnetic phase calculated by the LDA+U approach at zero temperature neglects the change of the entropy due to the variation of the spin and orbital configurations; the second one is that in the LDA+U approach and the present work the long-range orbital fluctuations are not taken into account.

C. Energy gap of single-particle spectra

In this subsection we study how the gap of single-particle energy spectra of the E$_g$ electrons depends on the evolution of the OO parameter. In the OO phase, the long-range orbital order breaks the symmetry of the orbital space, and opens an insulating gap Δ in single-particle excitation spectra of the TMO, forming an orbital insulator. Such an insulator differs from the single-band Mott-Hubbard insulators in many aspects. One of the outstanding characters is that the insulating gap strongly depends on the OO parameter, hence closely on the temperature. In the TMO with quarter filling, the tight-bonding spectrum of an E$_g$ electron reads:

$$
\begin{aligned}
H_t \;=\; & t \sum_{\langle i,j\rangle_{x,y}} \left[d^{\dagger}_{i1}d_{j1} \pm \sqrt{3}\left(d^{\dagger}_{i1}d_{j2} + d^{\dagger}_{i2}d_{j1} \right) + 3d^{\dagger}_{i2}d_{j2} \right] \\
& + 4t \sum_{\langle i,j\rangle_z} (d^{\dagger}_{i1}d_{j1} + h.c.)
\end{aligned}
\tag{3.5}
$$

where $d^{\dagger}_{i\gamma}$ creates a 3d electron at site i with orbital state γ; and $\pm$ denote the signs of the hopping integrals between two nearest-neighbor sites along the x and y direction, respectively. We ignore the spin index in the present FM GS.

Strong on-site Coulomb interaction U is the main character in these ordered TMO, that U >> t prohibits the E$_g$ electrons from double occupation at the same site, thus the single occupation constraint is applied on the E$_g$ orbits. In the limit of large Coulomb interaction, the constraint of no double occupancy at site R_i is enforced by introducing auxiliary fermions [26], $f^{\dagger}_{i\gamma}$, and bosons, b_i; here $f^{\dagger}_{i\gamma}$ creates a slaved fermion (electron) at site R_i with orbital state γ, and $b^{\dagger}_i$ creates a boson (hole) at site R_i, thus $d^{\dagger}_{i\gamma\sigma}=f^{\dagger}_{i\gamma\sigma}b_i$, and the single occupation condition is: $\sum_{\sigma\gamma} f^{\dagger}_{i\gamma\sigma}f_{i\gamma\sigma} + b^{\dagger}_i b_i = 1$. In the FM and G-AFO ordered phase, the effective

11

low-energy Hamiltonian becomes:

$$H_{eff} = \sum_k [\epsilon_k^{11} f_{k1}^\dagger f_{k1} + \epsilon_k^{22} f_{k2}^\dagger f_{k2} + \epsilon_k^{12}(f_{k1}^\dagger f_{k2}$$
$$+ f_{k2}^\dagger f_{k1}) + \tilde{J}_1(f_{k+Q,1}^\dagger f_{k2} + f_{k+Q,2}^\dagger f_{k1})]$$
$$+ \sum_k \lambda(f_{k1}^\dagger f_{k1} + f_{k2}^\dagger f_{k2} + b^2 - 1) \tag{3.6}$$

here $Q=(\pi,\pi,\pi)$, corresponding to the G-AFO order. The average of the boson occupation is approximated as a c-number: $< b_i^\dagger b_i >= x$. The dispersion functions are: $\epsilon_k^{11} = 4xt(\cos k_x + \cos k_y + 4\cos k_z) + 3\left(J_3 \langle s^z \rangle^2 + J_4\right)(\langle \tau^z \rangle + E_z/2)$, $\epsilon_k^{12} = 4\sqrt{3}xt(-\cos k_x + \cos k_y)$, and $\epsilon_k^{22} = 12xt(\cos k_x + \cos k_y) + 3(J_3 \langle s^z \rangle^2 + J_4)(\langle \tau^z \rangle + E_z/2)$. And the parameter $\tilde{J}_1 = -3\left(J_3 \langle s^z \rangle^2 + J_4\right)\langle \tau^x \rangle$. In the saddle-point approximation, the constraint constant λ and the boson occupation are:

$$\lambda = -\frac{1}{N}\sum_{\langle i,j\rangle\gamma\gamma'}\left(t_{ij}^{\gamma\gamma'}\left\langle f_{i\gamma}^\dagger f_{j\gamma'}\right\rangle + H\cdot C\right) \tag{3.7}$$

$$x = 1 - \frac{1}{N}\sum_i \left(\left\langle f_{i1}^\dagger f_{i1}\right\rangle + \left\langle f_{i2}^\dagger f_{i2}\right\rangle\right) \tag{3.8}$$

respectively. Physically λ shifts the energy level of the Fermi quasiparticles, and x gives rise to the hole concentration upon doping. In the compounds with quarter-filling, $x \to 0$. The single-quasiparticle energy spectra E_k have four branches and strongly depend on the OO parameter. For the G-AFO ordered TMO the lower two subbands are filled, since each magnetic and orbital unit cell contains two electrons at quarter-filling, the minimum of the empty subband separates from the maximum of the filled subbands by a gap Δ. This result considerably differs from Kilian and Khaliullian's gapless charge excitation [15]; in fact, in their study the modulation of the long-range OO on the motion of the electrons was not taken into account.

The thermal fluctuation weakens the OO parameter, hence softens the single-particle excitation spectra. The T-dependence of the energy gap of the single-particle spectra is shown in Fig.5. At low T, the strong Coulomb interaction of the 3d electrons, the large spatial anisotropy of 3d orbits and the crystalline field splitting cooperatively lift the orbital degeneracy, and favor the ordered orbital phase. The broken of the orbital space symmetry leads to that an electron must cost at least Δ in energy to hop to the nearest-neighbor site. Therefore the threshold Δ gives rise to the insulating gap of the TMO as an orbital
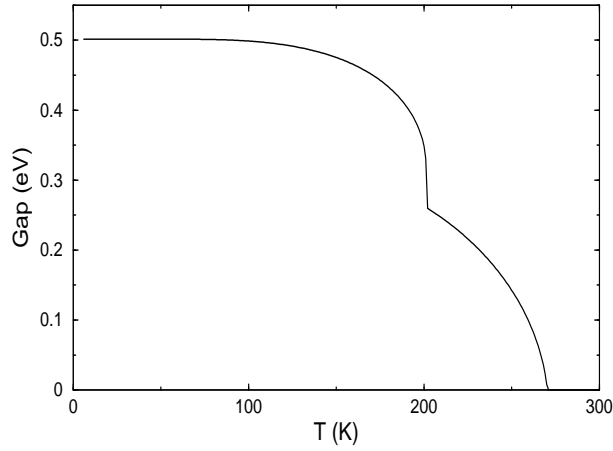
FIG. 5: Temperature dependence of the energy gap of the single-particle spectra in the ferromagnetic and G-type antiferro-orbital ordered phase. $\lambda = -0.1 eV$, and other parameters are the same to Fig.4.

insulator. This energy gap manifests in the optical excitation and transport, and differs from the energy gap of the orbital wave excitation. Increasing temperature gradually destroys the long-range OO, and leads to the decrease of the gap of the separated subbands. With the further increasing of temperature to $T = T_{OO}$, the thermal fluctuations become so strong that the long-range OO and the OO parameter vanish. In this situation, the two lower subbands merge together with the two higher subbands, the insulating gap disappears, see Fig.5, indicating the occurrence of MIT in TMO. Thus the energy gap of the orbital insulator crucially depends on the OO parameter, hence the temperature.

The temperature dependence of the insulating gap $\Delta(T)$ turns out to be similar to that of the OO parameter, steeply diminishes a fraction at the Curie temperature T_C and completely disappears at T_{OO}, see Fig.4 and Fig.5. Therefore, the temperature driven MIT in TMO is essentially induced by the orbital order-disorder transition. Our numerical results demonstrate the significant discrepancy between the optical and transport gap $\Delta(T)$ and the MIT critical temperature T_M. For the present system in Fig.5, the gap of the energy spectra, usually reflected in optical and transport experiments, is $\Delta = 0.5$ eV; while the MIT critical temperature $T_M = T_{OO} \approx 270K = 0.023$, which accounts for the considerable discrepancy between Δ and T_M in many orbital compounds.

13

IV. TEMPERATURE-DEPENDENT RESONANT X-RAY SCATTERING IN-TENSITIES

Strong interplay between spin and orbital degrees of freedom also manifests In the optical excitation of orbital insulating TMO. Recently it was proposed to utilizing the RXS technique to measure the OO phase by Murakami et $al.$ [28] for manganites and Fabrizio et $al.$ [29] for V_2O_3. The $1s - 3d$ K-edge RXS peak intensity is a useful signal to probe the OO phase and the orbital order-disorder phase transitions [11,27]. The polarization and azimuthal dependences of the RXS intensities provide the hidden information of the underlying OO parameters [27−30], and unveil the interplay between spins and orbits. Although the signal enhancement of the quadrupole $1s - 3d$ scattering (E_2) is less than that of the electric dipole $1s - 4p$ scattering (E_1), the observed E_2 spectral line shape as a function of energy is more easy to be identified than the quite complicated line shapes associated with E_1 process [11,28,29]. In what follows we present the E_2 RXS intensity and its evolution with temperature based on the OO phase obtained in the preceding section.

In the FM and G-AFO phase, the ordered 3d orbits in the sublattices consist of two different orbital basis: $|\psi_1\rangle = \alpha_1|1\rangle + \alpha_2|2\rangle$ and $|\psi_2\rangle = \alpha_1|1\rangle - \alpha_2|2\rangle$, here the coefficients α_1, α_2 are the functions of the interaction parameters. There exist two kinds of reflections: the fundamental reflection at $(hkl) = (n_x n_y n_z)$ and the orbital superlattice reflection at $(hkl) = \left(n_x + \frac{1}{2}, n_y + \frac{1}{2}, n_z + \frac{1}{2}\right)$. At the lattice symmetry-forbidden direction in which (hkl) are all odd, the orbital structure factor is written as:

$$\begin{aligned} F_{hkl} = & -8\sqrt{3}f\left(\Gamma, r_{2,ds}, c, \omega\right)\sqrt{n_{\epsilon k}n_{\epsilon' k'}}\langle\tau_x\rangle[\epsilon_z k_z \\ & \left(\epsilon'_x k'_x - \epsilon'_y k'_y\right) + \left(\epsilon_x k_x - \epsilon_y k_y\right)\epsilon'_z k'_z] \end{aligned} \tag{4.1}$$

where the function $f\left(\Gamma, r_{2,ds}, c, \omega\right)$ is the coefficient depending on the lifetime of the intermediate states, Γ, the radial matrix element $r_{2,ds}$, the velocity of photon c and the incoming photon frequency ω; $n_{\epsilon(\epsilon'),k(k')}$ is the density of the incoming (outgoing) beam of photons with polarization $\vec{\epsilon}\left(\vec{\epsilon'}\right)$ and wavevector $\vec{k}\left(\vec{k'}\right)$. When the incoming beam is perfect σ-polarized, the orbital structure factor for unrotated $(\sigma\sigma')$ channel is:

$$\begin{aligned} F_{\sigma\sigma'} = & \sqrt{\frac{n_{k\epsilon_k}n_{k'\epsilon_{k'}}}{3}}f(\Gamma, r_{2,ds}, c, \omega)\langle\tau_x\rangle[3\cos^2\theta(\sin^2 2\varphi \\ & - \sin 4\varphi) + 8\sin^2\theta(\sin^2\varphi\sin 2\varphi)] \end{aligned} \tag{4.2}$$

where θ and φ are the Bragg and the azimuthal angles, respectively. The azimuthal-angle and the temperature dependences of the RXS intensities at a selected azimuth angle of the OO superlattice Bragg reflection (111) are shown in Fig.6. A steep decrease of the RXS
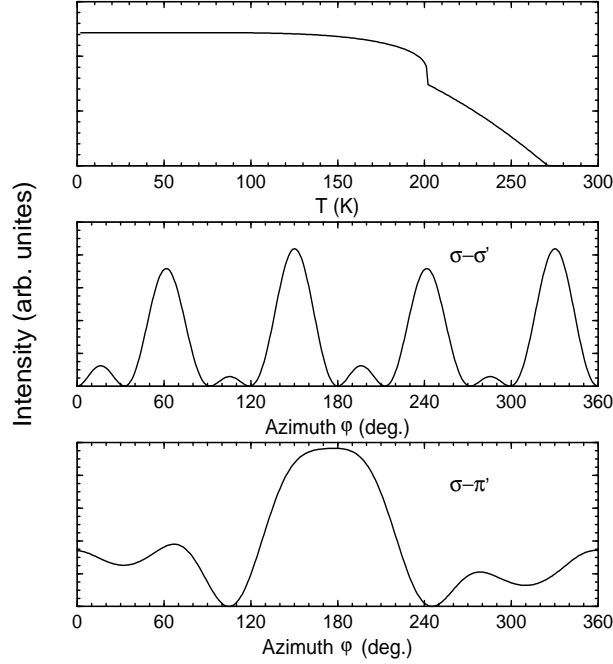

FIG. 6: Temperature (Fig.a) and azimuthal dependence of RXS intensities in the ferromagnetic and G-type orbital ordered phase in (111) direction for the unrotated ($\sigma\sigma'$) (Fig.b) and the rotated ($\sigma\pi'$) (Fig.c) channels.

intensities at T_C is observed in Fig.6. This discontinuous decrease is associated with the lost of magnetic order, which diminishes a fraction of orbital interaction. Such a discontinuous decrease is widely observed in the RXS experiments in manganites, $KCuF_3$ and YVO_3, a significant evidence of the strong spin-orbit coupling. The K-edge RXS peaks disappear completely at the OOT or MIT critical point. Therefore the RXS intensity could be a probe to the critical point of the MIT in orbital insulators.

V.   REMARKS AND SUMMARY

In the preceding sections we focus on the system with FM and G-AFO structure. For large U/J_H, the GS of the system is the A-AFM and G-AFO (C-AFO) ordered phase, as determined by the cluster-SCF approach. We find such an orbital ordered TMO also opens

an insulating gap in the single-particle energy spectra, and the energy gap exhibits similar dependences on the OO parameter and the temperature to those in the present paper. The dependence of the RXS intensity on temperature is also similar to the preceding result qualitatively, though the peak positions of the RXS intensities slightly shift in comparison with the present structure. Therefore different ordered orbital insulators share many common characteristics, and are significantly different from the conventional single-band Mott-Hubbard insulators [1,31].

Many cubic symmetric TMO with orbital degeneracy are inherently unstable, the orbital degeneracy is usually lifted by lowering the crystal symmetry through the JT distortions in LaMnO$_3$ [32] and YVO$_3$ [33], or other lattice distortion modes in V$_2$O$_3$ [16]. As far as the JT phonon-mediated orbital coupling is considered, an additional orbital-orbital interaction is introduced [9]:

$$\hat{H}_{JT} = \sum_{\langle ij_l \rangle}^{x,y,z} \frac{2g^2}{3K} I_i^l I_{j_l}^l \tag{5.1}$$

where g is the electron-phonon coupling constant, and K the restoring coefficient. For typical TMO in which JT effect plays a role, the parameters g $\sim$ 1.2 eV, and K $\sim$ 10.0 eV. In this situation, the orbital correlation arises from both the Coulomb interaction and the JT effect, thus the orbital GS is a combination of the pure electronic spin-orbital superexchange interaction and the crystalline field splitting described by Eq.(2) and the JT orbital interaction by Eq.(14). Utilizing the cluster-SCF method, we find that the most stable GS magnetic structure in this case is still FM and G-AFO ordering with a slight modification on the orbital occupation for small U/J_H; and for large U/J_H the GS is A-AFM and G-AFO ordering. Such system also exhibits most of characters of orbital insulators.

An obvious fact is that many OO insulators do not exhibit MIT when the long-range OO disappears at high temperature, such as in LaMnO$_3$ [34] and YVO$_3$ [33], except for V$_2$O$_3$. The essential reason is that these TMO are not simple orbital insulators, there also exists strong dynamic electron-phonon coupling, i.e., the dynamic JT effect, even if the static cooperative JT distortion disappears at high temperature. In these compounds, numerous dynamic JT phonons drag the motion of 3d electrons, and localize the 3d electrons as the incoherent polarons. The transport of the 3d electrons dragged by numerous dynamic phonons is of insulated polaronic character. Therefore these TMO are still insulators at high temperature. This addressed why T$_M \neq$ T$_{OO}$ in some compounds.

An important result from the preceding study is that the crystalline field splitting E_z plays crucial role for the stability of the OO GS. A pure spin-orbital interaction can not solely determine the magnetic and orbital GS, since the quantum fluctuation is large and the spin-orbital interacting system is still highly degenerate. The crystalline field splitting E_z may suppress the quantum fluctuation and drive the system into an stable GS. Similar result was also obtained by Fang and Nagaosa in the orbital compound YVO_3 in a recent paper [35].

In summary, in an orbital-degenerate spin-orbital interacting system, besides the orbital wave gap, an energy gap of the electronic excitation is opened as the orbital order develops, and disappears with the vanishing of the orbital order driven by the thermal fluctuations. The clear dependence of the insulating gap on the orbital order parameters shows that such TMO possesses the orbital insulator characters, and from which one could interpret the considerable discrepancy between the energy gap in the optical and transport experiments and the MIT critical temperature. The RXS intensity also exhibits the close interplay between spin and orbital orders. We expect more interesting properties of orbital insulator, such as the critical index near the transition point of the MIT, will be uncovered in the further studies.

Acknowledgments

[1] M. Imada, A. Fujimori and Y. Tokura, *Rev. Mod. Phys.* **70**, 1039 (1998).

[2] S. Jin, T. H. Tiefel, M. McCormack, R. A. Fastnacht, R. Ramesh and L. H. Chien, *Science*, **264**, 413 (1994).

[3] I. Loa, P. Adler, A. Grzechnik, K. Syassen, U. Schwarz, M. Hanfland, G. K. Rozenberg, P. Gorodetsky and M. P. Pasternak, *Phys. Rev. Lett.* **87**, 125501 (2001).

[4] For example, see Y. Tokura and N. Nagaosa, *Science* **288**, 462 (2000).

[5] G. A. Thomas, D. H. Rapkine, S. A. Carter, A. J. Millis, T. F. Rosenbaum, P. Metcalf and J. M. Honig, *Phys. Rev. Lett.* **73**, 1529 (1994).

[6] K. I. Kugel and D. I. Khomskii, *Sov. Phys.* JETP, **37**, 725 (1973).

[7] C. Castellani, C. R. Natoli and J. Ranninger, *Phys. Rev.* **B18**, 4945 (1978).

[8] D. I. Khomskii, *J. Mod. Phys.* **B15**, 2665 (2001).

[9] D. I. Khomskii and M.V. Mostovoy, *cond-mat/0304089*.

[10] Y. Tokura and N. Nagaosa, *Science*, **288**, 462 (2000).

[11] D. B. Mcwhan, J. P. Remeika, T. M. Rice, W. F. Brinkman, J. P. Maita and A. Menth, *Phys. Rev. Lett.* **27**, 941 (1971); *Phys. Rev.* **B7**, 1920 (1973).

[12] L. Paolasini, C. Vettier, F. de Bergevin, F. Yakhou, D. Mannix, A. Stunault, W. Neubeck, M. Altarelli, M, Fabrizio, P.A. Metcalf and J.M. Honig, *Phys. Rev. Lett.* **82**, 4719 (1999).

[13] Y. Endoh , K. Hirota, S. Ishihara, S. Okamoto, Y. Murakami, A. Nishizawa, T. Fukuda, H. Kimura, H. Nojiri, K. Kaneko and S. Maekawa, *Phys. Rev. Lett.* **82**, 4328 (1999).

[14] B. B. Van Aken, O. D. Jurchescu, A. Meetsma, Y. Tomioka and T.M. Palstra, *Phys. Rev. Lett.* **90**, 066403 (2003).

[15] R. Kilian and G. Khaliullin, *Phys. Rev.* **B60**, 13458 (1999).

[16] Liang-Jian Zou, M. Fabrizio and M. Altarelli, *preprint*.

[17] P. W. Anderson, *Phys. Rev.* **86**, 694 (1952).

[18] L. M. Roth, *Phys. Rev.* **146**, 306 (1966).

[19] M. Cyrot and C. Lyon-Caen, *J. Phys.* (Paris) **36**, 253 (1975).

[20] J. Kanamori, *J. Phys. Chem. Solids*, **10**, 87 (1959); J. B. Goodenough: *Phys. Rev.* **100**, 564 (1955).

[21] T. M. Rice, *Spectroscopy of Mott Insulators and Correlated Metals*, Eds. A. Fujimori and Y.

Tokura, (Springer-Verlag, Berlin Heidelberg 1995).

[22] H.-B. Tang, X.-F. Wei, D.-M. Chen and Liang-Jian Zou, *preprint.*

[23] For example, see N. Binggeli and M. Altarelli, *Phys. Rev.* **B70**, 085117 (2004).

[24] R. Caciuffo, L. Paolasini, A. Sollier, P. Ghigna, E. Pavarini, J. Van den Brink and M. Altarelli, *Phys. Rev.* **B65**, 174425 (2002).

[25] L. Paolasini, C. Vettier, F. de Bergevin, F. Yakhou, D. Mannix1, A. Stunault, W. Neubeck, M. Altarelli, M. Fabrizio, P. A. Metcalf, and J. M. Honig, *Phys. Rev. Lett.* **82**, 4719 (1999).

[26] N. Read and D. M. Newsn, *Solid State Commun.* **52**, 993 (1984).

[27] M. Altarelli, *Complementary between Neutron and Synchrotron X-Ray Scattering*, Ed. by A. Furrer, (World Scientific, 1998).

[28] Y. Murakami, H. Kawada, H. Kawata, M. Tanaka, T. Arima, Y. Moritomo and Y. Tokura: *Phys. Rev. Lett.* **80**, 1932 (1998).

[29] M. Fabrizio, M. Altarelli and M. Benfatlo, *Phys. Rev. Lett.* **80**, 3400 (1998); *ibid* **81**, E4030 (1998).

[30] S. Ishihara and S. Maekawa, *Phys. Rev.* **B58**, 13442 (1998).

[31] N. F. Mott, *Metal-Insulator Transitions*, (Taylor and Francis, London/Philadophia, 1990).

[32] E. Wollan and W. C. Koehler, *Phys. Rev.* **100**, 545 (1955).

[33] For example, see G. R. Blake, T. T.M. Palstra, Y. Ren, A. A. Nugroho and A. A. Mwnovsky, *Phys. Rev. Lett.* **87**, 245501 (2001).

[34] J. Geck, P. Wochner, D. Bruns, B. Buchner, U. Gebhardt, S. Kiele, P. Reutler, and A. Revcolevschi, *Phys. Rev.* **B69**, 104413 (2004).

[35] Zhong Fang and N. Nagaosa, *Phys. Rev. Lett.* **93**, 176404 (2004).